Volume 8, Issue 3, 2019, 643 - 648 **ISSN 2284-6808**

Letters in Applied NanoBioScience

www.NanoBioLetters.com

https://doi.org/10.33263/LIANBS83.643648

Original Research Article **Open Access Journal**

Received: 11.07.2019 / Revised: 22.08.2019 / Accepted: 25.08.2019 / Published on-line: 30.08.2019

Characterization of the biofield energy treated aluminium using PSA, PXRD, and TGA/DTG analytical techniques

Dahryn Trivedi [1], Mahendra Kumar Trivedi [1], Alice Branton [1], Gopal Nayak [1], Snehasis Jana [2, *]

[1]Trivedi Global, Inc., Henderson, USA
[2]Trivedi Science Research Laboratory Pvt. Ltd., Thane, India

*corresponding author e-mail address: ***publication@trivedieffect.com*** | Scopus ID: 7102102164

ABSTRACT

Aluminium is the most abundant metal and third most abundant element in the Earth's crust. This study was executed to determine the impact of the Trivedi Effect®-Consciousness Energy Healing Treatment on aluminium in terms of its physicochemical and thermal properties by using sophisticated analytical techniques. For the study, the test sample was divided into two parts and named as the control and treated sample. The control part was not given any treatment; while the treated part was given the Trivedi Effect®-Consciousness Energy Healing Treatment; named as Biofield Energy Treated sample and was done remotely by a renowned Biofield Energy Healer, Dahryn Trivedi. The particle sizes of the treated aluminium powder were significantly decreased at d_{10} (13.5%), d_{50} (12.07%), d_{90} (6.16%), and D(4, 3) {5.83%}, compared to the control sample. The specific surface area of the treated aluminium, as a result, was significantly increased by 16.67% than the control sample. The PXRD data revealed reduced peak intensities and crystallite sizes ranging from 5.10% to 10.73% and 5.89% to 23.13%, respectively, compared to the control sample. The average crystallite size of the treated aluminium was also decreased by 15.91% compared to the control sample. The onset temperature and maximum thermal degradation temperature (T_{max}) of the treated sample were increased by 7.41% and 3.76%, respectively, compared to the control sample. Thus, the thermal stability of the treated sample was increased as compared to the control sample. Hence, the overall analysis indicated the impact of the Trivedi Effect®-Consciousness Energy Healing Treatment on the physicochemical and thermal properties of aluminium as there might be the formation of a new polymorph that may show better solubility, absorption, and bioavailability along with improved thermal stability. The Trivedi Effect®-Consciousness Energy Healing Treated aluminium could be used efficiently in biomedical applications such as nanotubes in cancer therapy, biosensing, cell imaging, and nanoparticle formation for anti-microbial and anti-cancer activities, *etc*.

Keywords: *Aluminium, Consciousness Energy Healing Treatment, The Trivedi Effect®, PSA, PXRD, TGA/DTG.*

1. INTRODUCTION

Aluminium is the most abundant metal and third most abundant element in the Earth's crust. It is dull silver in appearance, soft, and light-weight metal; that happens due to the formation of a thin layer of oxidation on exposure to air [1]. There are various uses of aluminium oxide in the pharmaceutical and industrial manufacturing processes. It is used in these industries as desiccating agent, adsorbent, and catalyst, as well as the manufacturing of dental cement. There are various consumer products that use aluminium oxide such as, dispersing agent, abrasive in toothpaste, food additive, and in hemodialysis [2]. Besides, alumina (Al_2O_3), which is a type of bio-inert ceramics, is having good mechanical properties and resistance to wear and therefore used in the field of artificial bone, artificial joints, artificial auditory ossicle, artificial dental root, and bearing for artificial heart [3]. On the other hand, the aluminium oxide has been used these days in the formation of nanoparticles (AlNPs) and has been widely used in the biomedical applications. Some scientific studies reported the use of AlNPs in the form of ordered mesoporous aluminium oxide that helps in improving the oral delivery of anti-blood pressure drug Telmisartan as a poor-water soluble compound [4]. Aluminium oxide NPs has been also used to sense bovine serum albumin and therefore used in the biosensing technology. This application was based on the florescent nature of the aluminium oxide nanostructures and was used in different biodetection purposes such as intracellular cargo monitoring, cell imaging, and *in vitro* DNA detection [5]. Moreover, the aluminium oxide nanomaterial is also used in the form of nanotubes to target autophagy signalling in both the cancerous as well as normal human cells [6]. In addition to the use in cancer therapy, some studies also reported the anti-cancer properties of spherical nano-aluminium oxide particles [7]. Also, the AlNPs show strong anti-microbial activities due to the large surface area [8]. The alpha-AlNPs are used as anti-asthmatic nano-drug that acts by conjugating with vasoactive intestinal peptide and therefore helps in treating allergic asthma in the mouse model [9]. Besides, some studies were also done on aluminium for its biological function that proposed its significant role in biomolecular compaction due to its abundance, high charge density metal cation nature. The research also suggests the use of specific consequence of aluminium biocompaction in the condensation of A+ T-rich chromatin domains, as well as in silencing the expression of some specific genetic information [10].

Several scientific studies reported the importance of physicochemical and thermal properties of drugs and adjuvant in the formulation development and main emphasis of research studies in these days are on achieving the maximum efficacy of

the drug by altering such properties [11]. The Consciousness Energy Healing Treatment is such kind of a novel approach that has been used by various scientists to modify the physicochemical and thermal properties of compounds and thereby attaining maximum biological activity [12, 13]. The human body is known to be surrounded by electrical currents, along with their associated magnetic fields [14]. Besides, the human body eliminates a broad spectrum of radiant energies *i.e.,* electromagnetic waves, ranging from the ultra-low, low, and infrared rays [15]. Therefore, an expert has the ability to transmit the energy to any living organism(s) or non-living object(s) around the globe by harnessing it from the universe. The object or recipient that receives the Biofield Energy always responds in a useful way. This process is known as the Trivedi Effect®-Biofield Energy Healing Treatment [16, 17]. Various research studies reported the use of Energy Therapy against different diseases due to their advantageous effect under the field of Complementary and Alternative Medicine (CAM) therapies and such therapies are also accepted by the National Center for Complementary and Alternative Medicine (NCCAM) along with other therapies, i.e., yoga, Ayurveda, Reiki, etc. [18, 19]. Similarly, the Trivedi Effect®-Consciousness Energy Healing Treatment has been known for its significant impact on the living organisms and non-living materials such as, in the field of antimicrobial activity [20-22], agricultural productivity [23, 24], metals, ceramics, and chemicals [25-27], pharmaceuticals/nutraceuticals [28-30], biotechnology [31, 32], cancer research [33], and skin and bone health [34-36], *etc*. Therefore, this research work was designed with the aim to identify the effect of the Biofield Energy Treatment on the physicochemical and thermal properties of aluminium by using various analytical techniques.

2. EXPERIMENTAL SECTION

2.1. Chemicals and Reagents.

The test sample aluminium powder was purchased from Parshwamani Metals, Mumbai, Maharashtra, India. Similarly, all other chemicals used in the experiments were purchased in India.

2.2. Consciousness Energy Healing Treatment Strategies.

The experimental design includes dividing the aluminium sample into two parts, among which the first part was not provided the Biofield Energy Treatment, and called a control sample. Besides, the second part of the sample was exposed to the Trivedi Effect®-Energy of Consciousness Healing Treatment for 3 minutes under the laboratory conditions and known as The Biofield Energy Treated sample. This Treatment was provided to the test sample, remotely, by the renowned Biofield Energy Healer, Dahryn Trivedi, USA, through the unique energy transmission process. Then, the control sample was treated by a "sham" healer, who did not have any understanding about the Biofield Energy Treatment. The samples were then stored in sealed conditions and characterized further by using different analytical techniques.

2.3. Characterization.

The particle size distribution (PSD) analysis of aluminium powders was performed with the help of Malvern Mastersizer 2000 (UK) using the wet method [37, 38]. The powder X-ray diffraction (PXRD) analysis of aluminium powder sample was performed by Rigaku MiniFlex-II Desktop X-ray diffractometer (Japan) [39, 40]. The crystallites size was calculated from PXRD data using the Scherrer's formula (1)

$$G = k\lambda/\beta\cos\theta \quad (1)$$

Where G is the crystallite size in nm, k is the equipment constant, λ is the radiation wavelength, β is the full-width at half maximum, and θ is the Bragg angle [41].

Similarly, the thermal gravimetric analysis (TGA) thermograms of aluminium powder were obtained with the help of TGA Q50 TA instruments [42].

The % change in particle size, specific surface area (SSA), peak intensity, crystallite size, and the maximum thermal degradation temperature (T_{max}) of the treated aluminium was calculated compared with the control sample using the following equation 2:

$$\%\ \text{change} = \frac{[\text{Treated} - \text{Control}]}{\text{Control}} \times 100 \quad (2)$$

3. RESULTS SECTION

3.1. Particle Size Analysis (PSA).

The changes in the particle size distribution of the treated aluminium powder after the Biofield Energy Treatment in comparison to the control sample was analyzed and the results were presented in Table 1. The analysis showed that the particle sizes of the treated sample were significantly decreased at d_{10} (13.5%), d_{50} (12.07%), d_{90} (6.16%), and D(4, 3) {5.83%}, compared to the control sample (Table 1). Thus, it indicated the higher impact of the Energy Treatment on the smaller sized particles than the larger particles of the treated aluminium. Besides, the specific surface area of the treated aluminium was observed to be increased significantly by 16.67% after the Biofield Energy Treatment that resulted due to the reduced particle size values of the treated aluminium, compared to the control sample.

Table 1. Particle size distribution of the control and treated aluminium.

Parameter	d_{10} (µm)	d_{50} (µm)	d_{90} (µm)	D(4,3)(µm)	SSA(m^2/g)
Control	11.93	36.12	95.00	47.35	0.24
Biofield Energy Treated	10.32	31.76	89.15	44.59	0.28
Percent change* (%)	-13.50	-12.07	-6.16	-5.83	16.67

d_{10}, d_{50}, and d_{90}: particle diameter corresponding to 10%, 50%, and 90% of the cumulative distribution, D(4,3): the average mass-volume diameter, and SSA: the specific surface area. *denotes the percentage change of the treated aluminium powder compared to the control sample.

In recent days, the use of nanoparticles has been evident as the drug delivery vehicles as well as direct targeting systems; however, they need to be properly designed for achieving the maximum efficacy. Any significant change in any property of nanoparticle such as particle size may affect the pharmacokinetics or therapeutic efficacy of the particle [43, 44]. Thus, it could be anticipated that the altered particle size and surface area of the treated aluminium sample might affect its use in the biomedical technologies such as fabrication of nanoparticles, direct targeting of cancerous cells, *etc*., as compared to the control sample.

3.2. Powder X-ray Diffraction (PXRD) Analysis.

The PXRD diffractograms were shown in Figure 1; while the comparative analysis of the peak intensities and crystallite sizes of both the samples were shown in Table 2. The diffractograms of the control and treated samples showed sharp and distinct peaks, thereby representing their crystalline nature; however, some variations were observed in the treated sample, compared to the control sample (Table 2).

Table 2. PXRD data for the control and treated aluminium.

Entry No.	Bragg angle (°2θ)		Intensity (cps)			Crystallite size (G, nm)		
	Control	Treated	Control	Treated	% Change*	Control	Treated	% Change*
1	38.47	38.20	1128	1015	-10.02	595	465	-21.85
2	44.72	44.47	550	491	-10.73	588	452	-23.13
3	65.07	64.85	307	282	-8.14	613	532	-13.21
4	78.02	77.97	353	335	-5.10	611	575	-5.89

*denotes the percentage change of the treated aluminium compared to the control sample.

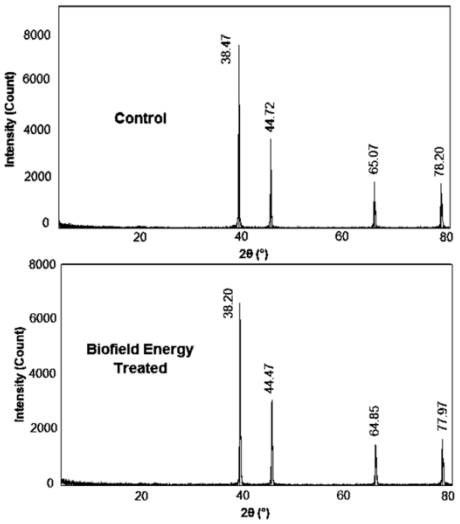

Figure 1. PXRD diffractograms of the control and treated aluminium.

Besides, the peak intensities corresponding to the characteristic peaks of the treated sample as well as their crystallite sizes also showed significant changes. The treated sample showed a reduction in the peak intensities and crystallite sizes in the range from 5.10% to 10.73% and 5.89% to 23.13%, respectively, compared to the control sample. Also, the Biofield Energy Treatment affected the average crystallite size of the treated sample (506.00 nm) that was significantly reduced by 15.91% than the control sample (601.75 nm). Some scientific studies reported that the alterations in the crystal properties such as Bragg's angles of the peaks present in diffractogram and their peak intensities and crystallite sizes might indicate the possible formation of new polymorph that may affect the solubility and bioavailability profile of the drug [45, 46]. Therefore, the altered crystal properties of the treated sample after the Biofield Energy Treatment suggested some changes in the polymorphic properties that may improve its solubility and bioavailability profile as compared to the control sample.

3.3. Thermal Gravimetric Analysis (TGA)/ Differential Thermogravimetric Analysis (DTG).

TGA analysis helps in determining the weight change of a material as a function of increasing temperature. The aluminium powder is generally available in a gray coloured form due to the presence of oxide film on its surface. Therefore, the beginning of the thermal degradation of aluminium within 30-220°C involves the mass loss of 0.3% due to the oxidation of the surface particles [47].

Furthermore, the literature reported that heating the aluminium powder at the temperature more than 850°C resulted in a small increase in mass that was gradually increased at the temperatures of 1050, 1150, and 1250 °C. At temperatures of 1350 °C and above, the loss in mass value started that became significant above the temperature of 1400 °C due to the vaporization of aluminium [48].

Table 3. DTG data of the control and treated samples of aluminium.

Sample	DTG (Temperature, °C)		
	Onset	Peak	Endset
Control	557.36	610.02	679.61
Biofield Energy Treated	598.64	632.98	675.82
% Change	7.41	3.76	-0.56

*denotes the percentage change of the treated aluminium compared to the control sample.

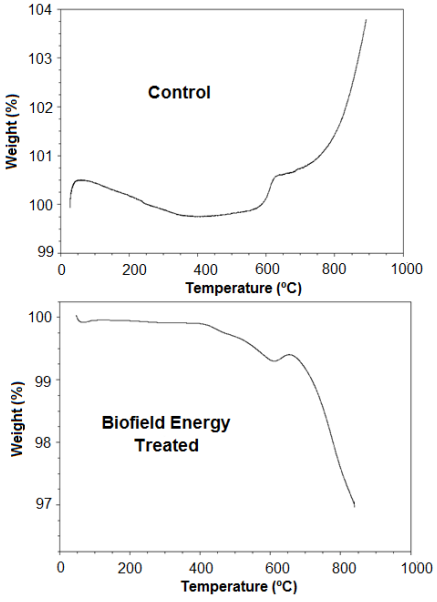

Figure 2. TGA thermograms of the control and treated aluminium.

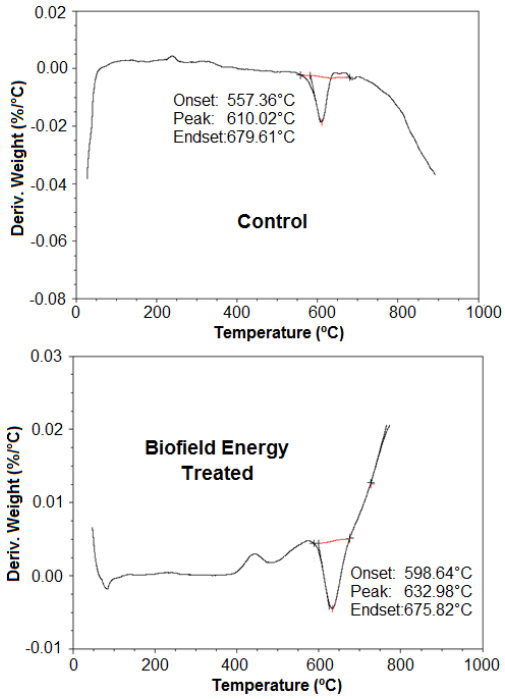

Figure 3. DTG thermograms of the control and treated aluminium.

In this study, the TGA/DTG analysis determines the effect of the Biofield Energy Treatment on the thermal properties of the treated aluminium sample in comparison to the control sample. The TGA thermograms of the control and treated samples were shown in Figure 2 in which, the thermogram of the control sample was observed similar as reported in the literature; whereas, the treated sample showed changes in the thermal degradation pattern.

Besides, the DTG analysis of both the samples was done to analyze the difference in the rate of thermal degradation and T_{max} of the treated sample as compared to the control sample (Figure 3). The onset temperature and T_{max} of the treated sample were significantly increased by 7.41% and 3.76%, respectively than the control sample; while the endset temperature was slightly reduced by 0.56% as compared to the control sample (Table 3). Thus, the DTG analysis indicated the significant increase in the thermal stability of the treated sample and the degradation pattern was also altered as observed in the TGA study, in comparison to the control sample. Overall, the TGA/DTG analysis indicated the increased thermal degradation pattern of the treated sample after the Biofield Energy Treatment as compared to the control aluminium sample.

4. CONCLUSIONS

The impact of the Trivedi Effect®-Consciousness Energy Healing Treatment was studied on the physicochemical and thermal properties of aluminium in comparison to the untreated sample. It was concluded that the particle sizes of the treated sample were significantly decreased at d_{10} (13.5%), d_{50} (12.07%), d_{90} (6.16%), and D(4, 3) {5.83%}, compared to the control sample. The specific surface area of the treated sample as a result, was significantly increased by 16.67% than the control sample. Such significant alterations shown in PSA and surface area analysis of the treated sample might indicate the improved solubility, absorption, and bioavailability of the sample when used in biomedical applications as compared to the untreated sample. The PXRD data revealed reduced peak intensities and crystallite sizes ranging from 5.10% to 10.73% and 5.89% to 23.13%, respectively, compared to the control sample. The average crystallite size of the treated sample was also decreased by 15.91% compared to the control sample. Such changes in the crystal properties of the treated sample might indicate the possible formation of new polymorph after the Biofield Energy Treatment as compared to the control sample. Such novel polymorph might show altered physicochemical and other properties as compared to the control sample that further may improve the use of the treated sample in the biomedical technologies. The onset temperature and T_{max} of the treated sample were increased by 7.41% and 3.76%, respectively, compared to the control sample. Thus, the results indicated the improved thermal stability of the treated sample than the control sample. Therefore, the study on the Biofield Energy Treated aluminium indicated the significant impact of the Trivedi Effect®-Consciousness Energy Healing Treatment on the physicochemical and thermal properties that might help in changing the solubility, bioavailability, and thermal stability of the treated sample than the control sample. Hence, the use of Biofield Energy Treatment as a novel approach of altering the properties of aluminium might be proved as beneficial in its biomedical application and product development such as biosensing, nanotube formation in cancer therapy, cell imaging, and nanoparticle formation for anti-microbial and anti-cancer activities, *etc*.

5. REFERENCES

1. Kretsinger, R.H.; Uversky, V.N.; Permyakov, E.A. Aluminum in Biological Systems. *Encyclopedia of Metalloproteins*. Springer, New York, 2013; https://doi.org/10.1007/978-1-4614-1533-6_105.

2. Krewski, D.; Yokel, R.A.; Nieboer, E.; Borchelt, D.; Cohen, J.; Harry, J.; Kacew, S.; Lindsay, J.; Mahfouz, A.M.; Rondeau, V. Human health risk assessment for aluminium, aluminium oxide, and aluminium hydroxide. *J Toxicol Environ Health B Crit Rev* **2007**, *10*, 1-269, https://doi.org/10.1080/10937400701597766.

3. Milne, I.; Ritchie, R.O.; Karihaloo, B.L. *Comprehensive Structural Integrity*, Elsevier, 2003.

4. Borbane, S.A.; Pande, V.V.; Vibhute, S.K.; Kendre, P.N.; Dange, V.U. Design and fabrication of ordered mesoporous alumina scaffold for drug delivery of poorly water soluble drug. *Austin Ther* **2015**, *2*, 2-6.

5. Tran, P.A.; Aramesh, M. Conformal nanocarbon coating of alumina nanocrystals for biosensing and bioimaging. *Carbon* **2017**, *122*, 422-427, https://doi.org/10.1016/j.carbon.2017.06.101.

6. Wang, Y.; Kaur, G.; Chen, Y.; Santos, A.; Losic, D.; Evdokiou, A. Bio-inert anodic alumina nanotubes for targeting of endoplasmic reticulum stress and autophagic signaling : a combinatorial nanotube-based drug delivery system for enhancing cancer therapy. *ACS Publ* **2015**, *7*, 27140-27151, https://doi.org/10.1021/acsami.5b07557.

7. Inbaraj, B.S.; Chen, B.H.; Rajan, Y.C. Synthesis and characterization of poly(γ-glutamic acid)-based alumina nanoparticles with their protein adsorption efficiency and

cytotoxicity towards human prostate cancer cells. *RCS Adv* **2015**, *5*, 15126, https://doi.org/10.1039/C4RA10445E.
8. Sadiq, I.M.; Chowdhury, B.; Chandrasekaran, N.; Mukherjee, A. Antimicrobial sensitivity of Escherichia coli to alumina nanoparticles. *Nanomed Nanotechnol Biol Med* **2009**, *5*, 282-286, https://doi.org/10.1016/j.nano.2009.01.002.
9. Athari, S.S.; Pourpak, Z.; Folkerts, G.; Garssen, J.; Moin, M.; Adcock, I.M.; Movassaghi, M.; Ardestani, M.S.; Moazzeni, S.M.; Mortaz, E. Conjugated alpha-alumina nanoparticle with vasoactive intestinal peptide as a nano-drug in treatment of allergic asthma in mice. *Eur J Pharmacol* **2016**, *791*, 811-820, https://doi.org/10.1016/j.ejphar.2016.10.014.
10. Lukiw, W.J. Evidence supporting a biological role for aluminum in chromatin compaction and epigenetics. *J Inorg Biochem* **2010**, *104*, 1010-1012, https://doi.org/10.1016/j.jinorgbio.2010.05.007.
11. Buckton, G.; Beezer, A.E. The relationship between particle size and solubility. *Int J Pharmaceutics* **1992**, *82*, 7-10, https://doi.org/10.1016/0378-5173(92)90184-4.
12. Branton, A.; Jana, S. The use of novel and unique biofield energy healing treatment for the improvement of poorly bioavailable compound, berberine in male *Sprague Dawley* rats. *American Journal of Clinical and Experimental Medicine* **2017**, *5*, 138-144.
13. Branton, A.; Jana, S. Effect of The biofield energy healing treatment on the pharmacokinetics of 25-hydroxyvitamin D_3 [25(OH)D_3] in rats after a single oral dose of vitamin D_3. *American Journal of Pharmacology and Phytotherapy* **2017,** *2*, 11-18.
14. Becker, R.O.; Selden, G. *The body electric: Electromagnetism and the foundation of life*, New York City, William Morrow and Company, 1985.
15. Barnes, R.B. Thermography of the human body. *Science* **1963**, *140*, 870-877, https://doi.org/10.1126/science.140.3569.870.
16. Trivedi, M.K.; Tallapragada, R.M.; Branton, A.; Trivedi, D.; Nayak, G. Spectral and thermal properties of biofield energy treated cotton. *American Journal of Energy Engineering* **2015**, *3*, 86-92.
17. Trivedi, M.K.; Patil, S.; Shettigar, H.; Bairwa, K.; Jana, S. Effect of biofield treatment on spectral properties of paracetamol and piroxicam. *Chem Sci J* **2015**, *6*, 98, https://doi.org/10.4172/2150-3494.100098.
18. Berman, J.D.; Straus, S.E. Implementing a research agenda for complementary and alternative medicine. *Annu Rev Med* **2004**, *55*, 239-254, https://doi.org/10.1146/annurev.med.55.091902.103657.
19. Barnes, P.M.; Bloom, B.; Nahin, R.L. Complementary and alternative medicine use among adults and children: United States, 2007. *Natl Health Stat Report* **2008**, *12*, 1-23.
20. Trivedi, M.K.; Branton, A.; Trivedi, D.; Nayak, G.; Charan, S. Phenotyping and 16S rDNA analysis after biofield treatment on *Citrobacter braakii*: A urinary pathogen. *J Clin Med Genom* **2015**, *3*, 129, http://dx.doi.org/10.4172/2332-0672.1000129.
21. Trivedi, M.K.; Patil, S.; Shettigar, H.; Mondal, S.C.; Jana, S. Evaluation of biofield modality on viral load of Hepatitis B and C viruses. *J AntivirAntiretrovir* **2015**, *7*, 083-088, https://doi.org/10.4172/jaa.1000123.
22. Trivedi, M.K.; Patil, S.; Shettigar, H.; Mondal, S.C.; Jana, S. An impact of biofield treatment: Antimycobacterial susceptibility potential using BACTEC 460/MGIT-TB System. *Mycobact Dis* **2015**, *5*, 189, https://doi.org/10.4172/2161-1068.1000189.
23. Trivedi, M.K.; Branton, A.; Trivedi, D.; Nayak, G.; Gangwar, M.; Snehasis, J. Agronomic characteristics, growth analysis, and yield response of biofield treated mustard, cowpea, horse gram, and groundnuts. *International Journal of Genetics and Genomics* **2015**, *3*, 74-80, https://doi.org/10.11648/j.ijgg.20150306.13.
24. Trivedi, M.K.; Branton, A.; Trivedi, D.; Nayak, G.; Mondal, S.C. Evaluation of plant growth, yield and yield attributes of biofield energy treated mustard (*Brassica juncea*) and chick pea (*Cicerarietinum*) seeds. *Agriculture, Forestry and Fisheries* **2015**, *4*, 291-295, http://dx.doi.org/10.5281/zenodo.192893
25. Trivedi, M.K.; Patil, S.; Tallapragada, R.M. Effect of biofield treatment on the physical and thermal characteristics of vanadium pentoxide powders. *J Material SciEng S* **2013**, *11*, 1, https://doi.org/10.5281/zenodo.192893.
26. Trivedi, M.K.; Branton, A.; Trivedi, D.; Nayak, G; Sethi, K.K.; Snehasis, J. Gas chromatography-mass spectrometry based isotopic abundance ratio analysis of biofield energy treated methyl-2-napthylether (Nerolin). *American Journal of Physical Chemistry* **2016**, *5*, 80-86, https://doi.org/10.11648/j.ajpc.20160504.11.
27. Trivedi, M.K.; Tallapragada, R.M.; Branton, A.; Trivedi, D.; Nayak, G.; Omprakash, L.; Snehasis, J. Characterization of physical and structural properties of aluminum carbide powder: Impact of biofield treatment. *J Aeronaut Aerospace Eng* **2015**, *4*, 142, https://doi.org/10.4172/2168-9792.1000142.
28. Trivedi, M.K.; Patil, S.; Shettigar, H.; Bairwa, K.; Jana, S. Effect of biofield treatment on spectral properties of paracetamol and piroxicam. *ChemSci J* **2015**, *6*, 98, https://doi.org/10.4172/2150-3494.100098.
29. Trivedi, M.K.; Patil, S.; Tallapragada, R.M.; Branton, A. Effect of Biofield Treatment on the Physical and Thermal Characteristics of Aluminium Powders. *Ind Eng Manage* **2014**, *4*, 151, https://doi.org/10.4172/2169-0316.1000151.
30. Trivedi, M.K.; Branton, A.; Trivedi, D.; Nayak, G.; Plikerd, W.D.; Surguy, P. A Systematic study of the biofield energy healing treatment on physicochemical, thermal, structural, and behavioral properties of magnesium gluconate. *International Journal of Bioorganic Chemistry* **2017**, *2*, 135-145.
31. Trivedi, M.K.; Patil, S.; Shettigar, H.; Bairwa, K.; Jana, S. Phenotypic and biotypic characterization of *Klebsiella oxytoca*: An impact of biofield treatment. *J MicrobBiochemTechnol* **2015**, *7*, 203-206, https://doi.org/10.4172/1948-5948.1000205.
32. Nayak, G.; Altekar, N. Effect of biofield treatment on plant growth and adaptation. *J Environ Health Sci* **2015**, *1*, 1-9, http://dx.doi.org/10.15436/2378-6841.15.001.
33. Trivedi, M.K.; Patil, S.; Shettigar, H.; Gangwar, M.; Jana, S. *In vitro* evaluation of biofield treatment on cancer biomarkers involved in endometrial and prostate cancer cell lines. *J Cancer SciTher* **2015**, *7*, 253-257, https://doi.org/10.4172/1948-5956.1000358.
34. Singh, J.; Trivedi, M.K.; Branton, A.; Trivedi, D.; Nayak, G.; Gangwar, M.; Snehasis, J. Consciousness energy healing treatment based herbomineral formulation: A safe and effective approach for skin health. *American Journal of Pharmacology and Phytotherapy* **2017**, *2*, 1-10.
35. Smith, D.M.; Trivedi, M.K.; Branton, A.; Trivedi, D.; Nayak, G. Sambhu, M.; Snehasis, J. Skin protective activity of consciousness energy healing treatment based herbomineral formulation. *Journal of Food and Nutrition Sciences* **2017**, *5*, 86-95, https://doi.org/10.11648/j.jfns.20170503.15.
36. Koster, D.A.; Trivedi, M.K.; Branton, A.; Trivedi, D.; Nayak, G.; Sambhu, M.; Snehasis, J. Evaluation of biofield

energy treated vitamin D_3 on bone health parameters in human bone osteosarcoma cells (MG-63). *Biochemistry and Molecular Biology* **2018**, *3*, 6-14, https://doi.org/10.11648/j.bmb.20180301.12.
37. Trivedi, M.K.; Sethi, K.K.; Panda, P.; Jana, S. A comprehensive physicochemical, thermal, and spectroscopic characterization of zinc (II) chloride using X-ray diffraction, particle size distribution, differential scanning calorimetry, thermogravimetric analysis/differential thermogravimetric analysis, ultraviolet-visible, and Fourier transform-infrared spectroscopy. *International Journal of Pharmaceutical Investigation* **2017**, *7*, 33-40.
38. Trivedi, M.K.; Sethi, K.K.; Panda, P.; Jana, S. Physicochemical, thermal and spectroscopic characterization of sodium selenate using XRD, PSD, DSC, TGA/DTG, UV-vis, and FT-IR. *Marmara Pharmaceutical Journal* **2017**, *21*, 311-318, https://doi.org/10.12991/marupj.300796.
39. Desktop X-ray Diffractometer "MiniFlex+". *The Rigaku Journal* **1997**, *14*, 29-36.
40. Zhang, T.; Paluch, K.; Scalabrino, G.; Frankish, N.; Healy, A.M.; Sheridan, H. Molecular structure studies of (1S,2S)-2-benzyl-2,3-dihydro-2-(1Hinden-2-yl)-1H-inden-1-ol. *J Mol Struct* **2015**, *1083*, 286-299, https://dx.doi.org/10.1016%2Fj.molstruc.2014.12.018.
41. Langford, J.I.; Wilson, A.J.C. Scherrer after sixty years: A survey and some new results in the determination of crystallite size. *J Appl Cryst* **1978**, *11*, 102-113, https://doi.org/10.1107/S0021889878012844.
42. Trivedi, M.K.; Branton, A.; Trivedi, D.; Nayak, G.; Plikerd, W.D.; et al. A systematic study of the biofield energy healing treatment on physicochemical, thermal, structural, and behavioral properties of iron sulphate. *International Journal of Bioorganic Chemistry* **2017**, *2*, 135-145.
43. Yu, X.; Trase, I.; Ren, M.; Duval, K.; Guo, X.; Chen, Z. Design of Nanoparticle-Based Carriers for Targeted Drug Delivery. *J Nanomater* **2016**, *2016*, 15, http://dx.doi.org/10.1155/2016/1087250.
44. Singh, R.; Lillard, J.W. Jr. Nanoparticle-based targeted drug delivery. *Exp Mol Pathol* **2009**, *86*, 215-223, https://doi.org/10.1016/j.yexmp.2008.12.004.
45. Trivedi MK, Branton A, Trivedi D, Nayak G, Lee AC, et al. Evaluation of the impact of biofield energy healing treatment (the Trivedi Effect®) on the physicochemical, thermal, structural, and behavioural properties of magnesium gluconate. *International Journal of Nutrition and Food Sciences* **2017**, *6*, 71-82, https://dx.doi.org/10.11648/j.ijnfs.20170602.13.
46. Savjani, K.T.; Gajjar, A.K.; Savjani, J.K. Drug Solubility: Importance and Enhancement Techniques. *ISRN Pharmaceutics* **2012**, *2012*, https://dx.doi.org/10.5402%2F2012%2F195727
47. Zhorin, V.A.; Kiselev, M.R.; Roldugin, V.I. Thermogravimetric analysis of the aluminium-polypropylene mixtures after plastic deformation under high pressure. *Russ J Appl Chem* **2013**, *86*, 15-19, http://dx.doi.org/10.1134/S1070427213010047.
48. Coker, E.N. The oxidation of aluminum at high temperature studied by Thermogravimetric Analysis and Differential Scanning Calorimetry. *Sandia National Laboratories California*, **2013**, https://doi.org/10.2172/1096501.

6. ACKNOWLEDGEMENTS

The authors are grateful to Central Leather Research Institute, SIPRA Lab. Ltd., Trivedi Science, Trivedi Global, Inc., Trivedi Testimonials, and Trivedi Master Wellness for their assistance and support during this work.

© 2019 by the authors. This article is an open access article distributed under the terms and conditions of the Creative Commons Attribution (CC BY) license (http://creativecommons.org/licenses/by/4.0/).